minerals

MDPI

Article

The Effects of Milling and pH on Co, Ni, Zn and Cu Bioleaching from Polymetallic Sulfide Concentrate

Jarno Mäkinen *, Tiina Heikola, Marja Salo and Päivi Kinnunen

VTT Technical Research Centre of Finland Ltd., 33101 Tampere, Finland; tiina.heikola@vtt.fi (T.H.); marja.salo@vtt.fi (M.S.); paivi.kinnunen@vtt.fi (P.K.)
* Correspondence: jarno.makinen@vtt.fi

Abstract: Acid bioleaching of a low-grade and polymetallic sulfide concentrate was studied, in order to determine suitable feed material particle size and pH for efficient leaching of valuable metals. The sulfide concentrate consisted of pyrite (50 wt %), pyrrhotite (31 wt %), quartz (10 wt %) and lower amounts of cobalt, nickel, zinc and copper (each <1 wt %). After adaptation of microorganisms in shake flasks, stirred tank tests were conducted at different pH levels and supplementing feed material at different particle sizes (milled to d80 < 150 µm, <50 µm, <28 µm, <19 µm). The operation at pH 1.8 was seen prone to iron precipitation, while this was not observed at a pH between 1.3 and 1.5. Additional milling to decrease particle size from the initial d80 < 150 µm had a major positive effect on cobalt- and nickel-leaching yields, proposing that at least d80 < 28 µm should be targeted. The best leaching yields for the main economic elements, cobalt and nickel, were 98% and 94%, respectively, reached with d80 < 19 µm at pH 1.3. However, it was considered that at pH 1.5, similar results could be obtained. This research sets the basis for continuing the experiments at a continuous pilot scale.

Keywords: bioleaching; pyrrhotite; pyrite; cobalt; nickel

Citation: Mäkinen, J.; Heikola, T.; Salo, M.; Kinnunen, P. The Effects of Milling and pH on Co, Ni, Zn and Cu Bioleaching from Polymetallic Sulfide Concentrate. *Minerals* **2021**, *11*, 317. https://doi.org/10.3390/min11030317

Academic Editor: Maxim Muravyov

Received: 17 February 2021
Accepted: 15 March 2021
Published: 18 March 2021

1. Introduction

Exhaustion of high-grade ores and an increasing demand of metals, especially cobalt and nickel in the battery sector, have attracted attention to polymetallic and/or low-grade deposits. Of the several considered technologies for utilizing these resources, bioleaching has gained particular interest, leading to various industrial-scale operations. For example, in Terrafame (Sotkamo, Finland), large but low-grade and polymetallic black schist ore is treated with heap bioleaching [1] At Mondo Minerals (Vuonos, Finland), a secondary stream of pentlandite ($(Fe,Ni)_9S_8$) and arsenopyrite (FeAsS) concentrate from a talc mine was treated [2], while Kasese Cobalt Company (Kasese, Uganda) utilized historic cobalt-bearing pyrite tailings [3]. In comparison to Terrafame, both the Vuonos and Kasese operations were utilizing stirred-tank bioleaching technology.

In all the above-mentioned industrial bioleaching operations, the leaching process relied on autotrophic microorganisms, i.e., lifeforms that obtain their carbon from inorganic substances such as CO_2. In the acidic bioleaching process, these chemolithotrophs can utilize supplemented oxygen to oxidize iron(II) to iron(III) form, which is known to be a strong oxidant [4]. Moreover, reduced or elemental sulfur species can be oxidized to sulfuric acid [5]. The biologically produced iron(III) and sulfuric acid will oxidize and dissolve iron-sulfide minerals, and more iron and sulfur is introduced to the leaching system. Eventually, the high concentration of iron(III) and acidity provides efficient oxidation for nearly all sulfide minerals, thus liberating their valuable metals into the leach solution [4,6]. As a conclusion, the benefits of the acid bioleaching technology are a low requirement of external chemicals or heat (as these are provided by the feed material itself in the exothermic leaching reactions), efficient nonselective leaching being especially useful for

polymetallic sulfide resources, and reduced gaseous sulfur emissions compared to the traditional concentrate roasting route [7].

When considering bioleaching of concentrates and tailings produced by froth flotation, mining and comminution activities have already taken place earlier, thus decreasing the associated processing costs [8]. Generally, flotation residues have a particle size of <100 μm [9]. It remains unclear how much additional milling is needed as mechanical activation to reach adequate bioleaching yields and kinetics in a stirred-tank process. It has been shown that by decreasing the particle size, the specific surface area increases, and leaching is enhanced both by kinetics and yields [10–12](Torma et al., 1972, Torma et al., 1977, Miller et al., 1999). However, results showing no clear benefits regarding additional milling have also been reported [13]. Moreover, too fine of a particle size has been considered inhibitory to bioleaching microorganisms (reviewed in [14,15]). On the other hand, bioleaching has been reported successful even with a particle size below 1 μm [16]. In the industrial stirred-tank bioleaching operations of Kasese and Vuonos, additional milling was utilized to reach d80 <35 μm and <20 μm particle size, respectively [2,3]. Thus, it can be concluded that additional milling depends at least on the feed material's mineralogy and liberation, the used microorganisms and additional costs related to the pretreatment.

The aim of this research is to evaluate the possibility to use acid bioleaching for a polymetallic sulfide concentrate, containing large amounts of pyrite (FeS_2) and pyrrhotite ($Fe_{1-x}S$ (x = 0 to 0.2)), and minor amounts of cobalt, nickel, zinc and copper. The main studied parameter was the effect of additional milling, i.e., the suitable particle size for a stirred-tank system. For this objective, the used mixed microbial culture was adapted to polymetallic sulfide concentrate, and a suitable pH level for bioleaching was determined. Finally, the effects of additional milling on bioleaching were tested with the most suitable parameters. Generally, the "parameter suitability" was justified by the cobalt-leaching yield, as it was the most valuable element of the polymetallic sulfide concentrate.

2. Materials and Methods

2.1. Sample Material and Analytics

The studied sulfide concentrate was obtained from the operating ore concentrator plant, where ore processing included milling, flotation circuits for copper and zinc recovery and finally a residual sulfide flotation circuit to separate pyrite and pyrrhotite as sulfur concentrate from the nonsulfidic fraction. The received pyrite–pyrrhotite sulfidic concentrate sample was dried at room temperature to prevent oxidation of sulfides, and then homogenized by mixing. Sample milling was conducted by a Mergan ball mill with stainless steel balls with full 5 kg loadings of the sulfide concentrate. The mill space and used water were purged with N_2 gas to prevent oxidation of sulfides during milling. The resulting particle size was determined with a Beckman Coulter LS laser diffraction particle-size analyzer (Beckman Coulter, Brea, CA, USA). The milled samples were dried at room temperature, and dry samples were analyzed for mineralogy (MLA 600, which is built on Quanta 600 SEM made by FEI Company (now Thermo Fisher Scientific) equipped with MLA software version 3.1.4.686, Thermo Fisher Scientific Inc., Waltham, MA, USA), and elemental composition with sulfide-S content (XRF and Eltra, respectively) to determine if oxidation of sulfides or elemental losses took place. The sample homogenization, milling, particle size determinations, drying and above-mentioned analysis were subcontracted from Geological Survey of Finland (GTK). The used sulfide concentrate was not sterilized in experiments.

In the actual leaching studies, pH and RedOx potential were measured using a Consort multiparameter C3040 analyzer, with Van London-pHoenix Co. pH and RedOx electrodes (Ag/AgCl in 3 M KCl; pH electrode calibration 1.68/4.01/7.00; RedOx electrode calibration +650 mV). The Eh (SHE) value was calculated by adding +210 mV to the RedOx meter reading. The dissolved iron(III) concentration was determined by the EDTA (ethylenediaminetetraacetic acid) and 5-sulfosalicylic titration method, developed for polymetallic leachates [17]. The acid-dissolving total iron content of the bioleaching system was deter-

mined by mixing 10 mL of the reactor pulp with 2 mL of 37% HCl and agitating the pulp for 30 min in a beaker with a magnetic stirrer. Then, the leached pulp was filtrated with a 0.45 µm syringe-filter and the filtrate was analyzed with ICP-OES (inductively coupled plasma optical emission spectrometry). The elemental composition of solutions and solids was analyzed with ICP-OES (5100 SVDV, Agilent Technologies, Santa Clara, CA, USA). For ICP-OES analysis, solid samples were digested completely with microwave-assisted acid digestion (UltraWAVE, Milestone, Sorisole, Italy).

2.2. Microorganisms and Adaptation

The previously enriched mixed culture of bioleaching microorganisms originating from acidic mine waters was used. The culture contained *Marinobacter* sp., *Acidithiobacillus* spp. (*A. ferrooxidans*, *A. thiooxidans*, *A. albertensis*, *A. ferrivorans*), *Leptospirillum* sp. (*L. ferrooxidans*), *Cuniculiplasma* sp., *Nitrosotenius* sp. and *Ferroplasma* sp. [18,19]. The adaptation of the mixed culture took place in 250 mL shake flasks in an orbital shaker (Stuart SI-500; 35 °C, 150 rpm) by mixing 90 mL of nutrient medium (Table 1), 22 g/L of $FeSO_4 \cdot 7H_2O$, 10 g/L of S_8 and 10 mL of active mixed microbial culture and sulfide concentrate sample. The pH was maintained at <2.0 by manually adding 4 M H_2SO_4. If spontaneous pH decrease and Eh increase were observed, the obtained culture was reinoculated with increased sulfide concentrate mass. This was continued until the culture was adapted to a 50 g/L solid/liquid ratio (S/L). Then, $FeSO_4 \cdot 7H_2O$ and S_8 additions were ended and the adapted culture was incubated and maintained only in the presence of nutrient medium (Table 1) and sulfide concentrate sample (50 g/L).

Table 1. Nutrient medium used in experiments ([20] without iron).

Compound	Concentration (g/L)
$(NH_4)_2SO_4$	3.0
K_2HPO_4	0.50
$MgSO_4 \cdot 7H_2O$	0.50
KCl	0.10
$Ca(NO_3)_2 \cdot 4H_2O$	0.014

2.3. Stirred-Tank Bioleaching Tests

The stirred-tank bioleaching experiments were conducted in 1 L glass reactors equipped with baffles and a heated water jacket. Agitation was provided by an overhead stirrer (300 rpm) and a single-shaft impeller system with a Rushton turbine near the reactor bottom, and the blade impeller in the mid-height of the reactor. Aeration (normal air, 1 L/min) was supplemented to the bottom-center of the reactor, from below the Rushton turbine. The experimental list is shown in Table 2.

Table 2. Parameters of the bioleaching reactor (BR) tests.

Experiment	Target pH	Particle Size, d80 < (µm)
BR1	1.8 ± 0.2	19
BR2	1.5 ± 0.2	19
BR3	1.3 ± 0.2	19
BR4	1.3 ± 0.2	19
BR5	1.3 ± 0.2	28
BR6	1.3 ± 0.2	50
BR7	1.3 ± 0.1	150

All reactors were ramped up by mixing 640 mL of nutrient medium (Table 1), 160 mL of active adapted microbial culture and 44 g/L of $FeSO_4 \cdot 7H_2O$. The active culture inoculum for the tests was grown in a reactor apparatus similar to the description above, and the same growth batch was used as inoculum per a test series (either pH or particle size). Thus, the

inoculation was identical per test series to allow reliable comparison of the single-parameter effect. However, as the inoculum was not from the same batch regarding different test series, comparison between the different parameters to each other was considered less reliable.

The reactors were operated at 35 °C with aeration. When added iron was oxidized and Eh exceeded +890 mV, 40 g (50 g/L) of dry sulfide concentrate was added to the reactors. After material addition, the pH was manually fixed to 1.3, 1.5 or 1.8 with 4 M H_2SO_4. When the Eh reached +810 mV, the ramp-up was finished and the actual bioleaching test was conducted for 7 days. This protocol was used to overcome the initial pyrrhotite-related acid consumption, allowing us to then monitor bioleaching of pyrite and other cobalt-bearing minerals with identical retention times at Eh values representing continuous-mode operations. During the actual bioleaching tests, the pH was controlled by continuously pumping $CaCO_3$ slurry to the reactors (the slurry concentration varied from 0 to 50 g/L due to adjusting the dosage to the available pumping speeds and reactor volume). Bioleaching reactors were monitored daily and pH and water levels were adjusted, if needed, with $CaCO_3$, 4 M H_2SO_4 and ddH_2O.

3. Results

3.1. Sample Material and Particle-Size Reduction

The results of elemental and mineralogical analysis are shown in Tables 3 and 4, respectively. According to the elemental analysis, sulfur was nearly completely in sulfide form. According to the in situ values of metals, the primary economic objective was on cobalt leaching (Figure 3). The mineralogical analysis revealed that the sulfide concentrate was dominated by pyrite and pyrrhotite, and to a lesser extent by quartz. Cobalt was incorporated into the pyrite matrix, but also present in various other sulfide minerals, similar to nickel. Copper and zinc were found mainly from their sulfide minerals of chalcopyrite and sphalerite, respectively. The amount of neutralizing minerals was very low.

Table 3. Elemental composition of the sulfide concentrate (ICP-OES, except * Eltra). The in situ value was calculated as US dollars per one ton of sulfide concentrate (cash-offer prices on 15 December 2020 by [21]). n.a. = not available.

Element	Concentration (wt %)	In-Situ Value (USD/t)
Fe	39.8	n.a.
S	38.4	n.a.
sulfide-S *	37.8	n.a.
Si	2.02	n.a.
Ca	1.02	n.a.
Zn	0.76	21
Co	0.70	222
Cu	0.53	41
Mg	0.52	n.a.
Ni	0.374	66
Al	0.167	n.a.
As	0.097	n.a.
Mn	0.0711	n.a.
Na	0.0388	n.a.

Table 4. Mineralogical composition of the sample (analyzed with MLA 600).

Mineral	Equation	Concentration (wt %)
Pyrite	FeS_2	49.9
Pyrrhotite	$Fe_{1-x}S$ (x = 0 to 0.2)	31.1
Quartz	SiO_2	10.0
Tremolite	$Ca_2(Mg_{5.0–4.5}Fe^{2+}{}_{0.0–0.5})Si_8O_{22}(OH)_2$	1.8
Chalcopyrite	$CuFeS_2$	1.2
Sphalerite	(Zn,Fe)S	1.2
Dolomite	$CaMg(CO_3)_2$	1.0
Calcite	$CaCO_3$	0.7
Linnaeite_polydymite	$Co^{2+}Co_2{}^{3+}S_4$ to $Ni^{2+}Ni_2{}^{3+}S_4$	0.5
Plagioclase	$NaAlSi_3O_8$–$CaAl_2Si_2O_8$	0.5
Pentlandite_Co	$(Co,Ni,Fe)_9S_8$	0.4
Talc	$Mg_3Si_4O_{10}(OH)_2$	0.4
Phlogopite	$KMg_3(AlSi_3O_{10})(F,OH)_2$	0.4
Cobaltite	CoAsS	0.2
Pentlandite	$(Fe,Ni)_9S_8$	0.1
K_feldspar	$KAlSi_3O_8$	0.1
Unknown		0.5
Total		100.0

The effects of milling time on particle size and sulfide-S loss are reported in Table 5. Both sulfide-S and total-S concentration had a slowly decreasing trend when milling time was increased, reaching the maximal sulfide loss of 2 wt % at d80 < 19 µm. According to the XRF analysis from the milled fractions, other elements did not have a similar decreasing trend in concentration or major changes (data not shown). As sulfide loss was minor, and no changes in metal concentrations were encountered, obtained milled fractions were concluded to be representative for the scope of the study.

Table 5. Milling time with resulting particle size and sulfur species concentration (Eltra).

Milling Time (min)	Particle Size (d80 <µm)	Particle Size (d10 <µm)	Sulfide-S (wt %)	Total-S (wt %)
0 (native)	150	23.4	37.8	38.6
60	50.3	7.67	36.5	37.3
120	28.1	3.24	36.3	37.3
200	19.5	1.68	35.8	37.0

3.2. Stirred-Tank Bioleaching Tests

Generally, the pH control during the ramp-up phase intended for pyrrhotite oxidation was challenging. Despite the H_2SO_4 additions, the pH peaked easily from the target level (pH 1.3, 1.5, 1.8) to pH 2.0–2.5. In addition to manual H_2SO_4 dosing, automatic titrators were tested, but were considered even more unreliable due to clogging of electrodes during the night. Nevertheless, after the ramp-up, the pH was easier to control and was in line with the data shown in Table 2.

Regarding the different operating pH levels in bioleaching, the resulting Eh and iron(III) concentrations are shown in Figure 1. The longest ramp-up phase was observed with BR1, which was also the most challenging in terms of pH control (the pH fluctuated between target pH 1.8 and pH 2.5 on days –5 and –4; with a final peak of pH 2.2 on day –3). The BR2 had a pH peak of pH 2.4 on day –3, and of pH 2.1 on day –1. BR3 had a pH peak on day –2 (pH 1.9) and day –1 (pH 1.7). Regarding the BR1, iron(III) concentration collapsed during the ramp-up (day –3) and at the end of bioleaching (day 7). To understand the iron behavior, total acid dissolving iron for BR1 was added to Figure 1. The total iron in leachate was 12.4 g/L and 5.3 g/L on days –3 and 7, respectively, while on other days all iron forms were close to each other. Thus, on day –3, iron was not precipitated, but present

mainly as iron(II), while on day 7, approximately 67% of iron(III) precipitated. For BR2 and BR3, concentrations of iron(III), total acid dissolving iron and total iron in the leachate were similar per measurement points throughout the tests. Thus, there seemed not to be major iron(III) precipitations or presence of iron(II) in tests operated at lower pH.

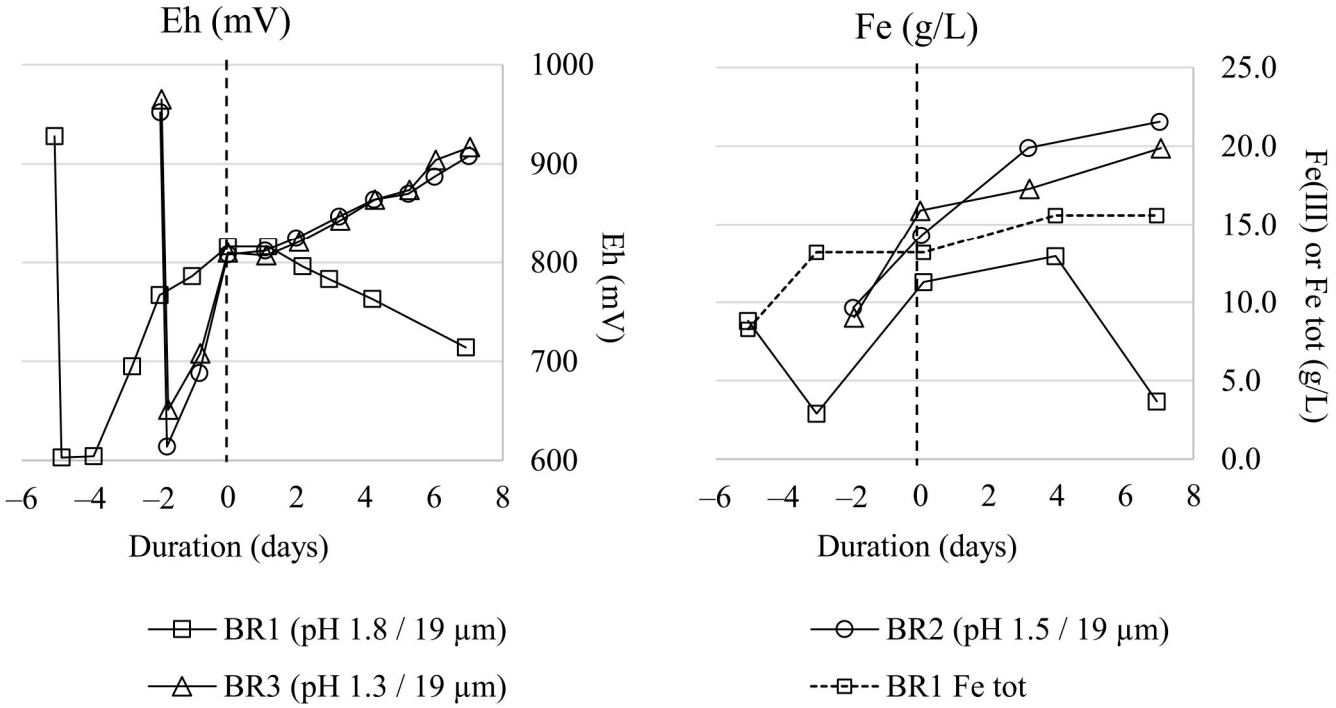

Figure 1. Evolution of Eh, Fe(III) and total acid dissolving Fe (only for BR1) concentration in bioleaching reactors with different operating pH values. The dashed vertical line illustrates the starting point of 7-day bioleaching tests. The negative days illustrate the length of ramp-up phase.

Regarding the different sulfide-concentrate particle sizes in bioleaching, the resulting Eh and iron(III) concentrations are shown in Figure 2. The longest ramp-up phase was observed with BR5 and BR6. Both these reactors had some elevated pH peaks during the ramp-up; BR5 on day –7 (pH 1.9) and BR6 on day –6 (pH 1.7). BR5 had also a collapse of pH on day –4 (pH 1.0). For BR7, elevated pH peaks occurred later, on day –1 (pH 1.8) and day 0 (pH 1.7). BR4 had no major pH peaks during the operation. Regarding BR5 and BR6, total acid dissolving iron concentration did not collapse during the ramp-up, compared to iron(III) concentration (Figure 2). Thus, iron was not precipitated, but present mainly as iron(II). For BR4 and BR7 concentrations of iron(III), total acid dissolving iron and total iron in the leachate were similar per sampling point throughout the tests, signaling that no major iron(III) precipitations took place during the tests. This also applied to BR5 and BR6 for the actual bioleaching period after the ramp-up.

Consumption of chemicals is presented in Table 6. The acid consumption took place mainly during the ramp-up phase, while $CaCO_3$ was consumed during the actual bioleaching operation.

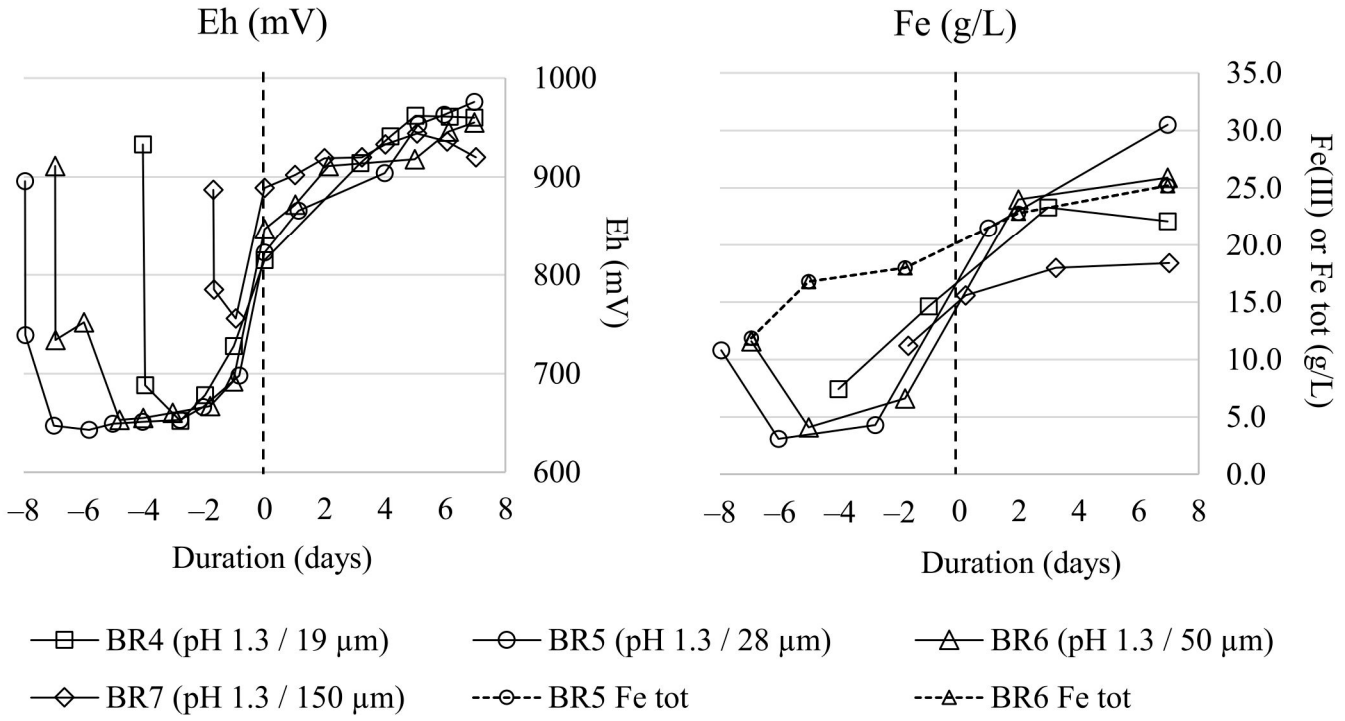

Figure 2. Evolution of Eh, Fe(III) and total acid dissolving Fe concentration (only for BR5 and BR6) in bioleaching reactors with different sulfide concentrate particle sizes (d80 <µm). The dashed vertical line illustrates the starting point of 7-day bioleaching tests. The negative days illustrate the length of ramp-up phase.

Table 6. The acid and base consumption in bioleaching tests, normalized to 95% H_2SO_4 and pure 100% $CaCO_3$ use per kg of feed material.

Experiment	Acid Consumption g/kg H_2SO_4	Base Consumption g/kg $CaCO_3$
BR1 (pH 1.8/19 µm)	277	839
BR2 (pH 1.5/19 µm)	346	814
BR3 (pH 1.3/19 µm)	568	595
BR4 (pH 1.3/19 µm)	427	756
BR5 (pH 1.3/28 µm)	513	645
BR6 (pH 1.3/50 µm)	534	573
BR7 (pH 1.3/150 µm)	315	50

Dissolution of metals (Figure 3) was calculated according to Equation (1)

$$Dissolution = \frac{(c_t - c_0) * V}{m} \quad (1)$$

where c_t is the concentration of an element on selected measurement point, c_0 is the concentration of an element before adding the sulfide concentrate sample (subtracted to notice the inoculum effect), V is the working volume of the reactor and m is the added solid sulfide concentrate. Generally, calculations based on leachates were problematic, as in an ongoing experiment reactor, leachate volume was not determined accurately (reactor surface was vivid due to active agitation and aeration). Moreover, the inoculum had some impact on leachate-based calculations between the test series (BR1–BR3 versus BR4–BR7). Thus, it was considered that the dissolution rate was only indicative and illustrated the leaching kinetics of target metals and revealed the leaching order of different sulfide minerals.

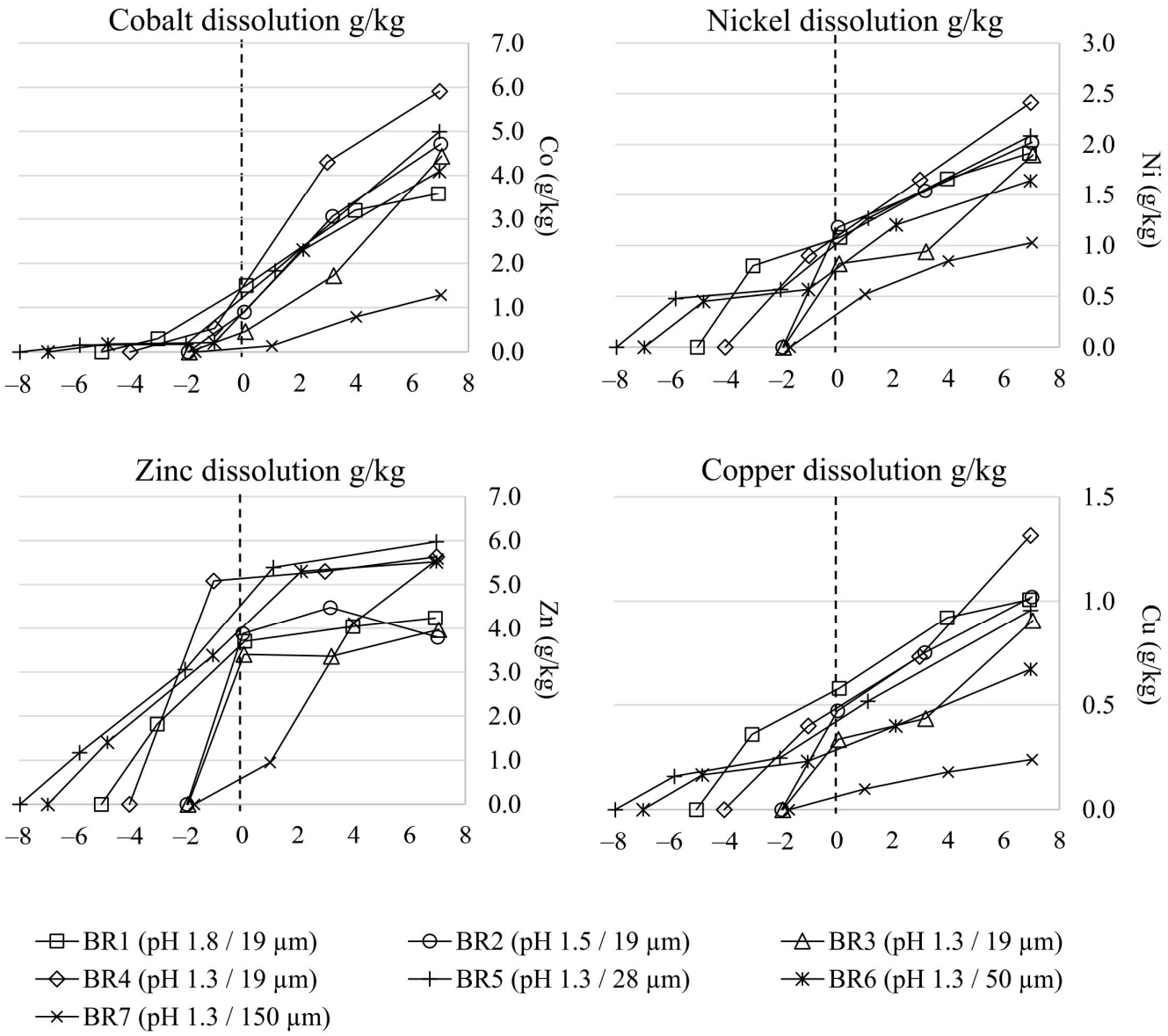

Figure 3. Metal dissolutions expressed as metals dissolved (grams) per sulfide concentrate added (kg). The horizontal axis represents leaching days (negative days were the ramp-up; positive days were the actual operation).

Leaching yields of metals (Figure 4) were calculated according to Equation (2):

$$Leaching\ yield\ = \left(1 - \frac{c_f * m_f}{c_0 * m_0}\right) * 100\% \quad (2)$$

where c_f is the concentration of an element in leach residue, m_f is the dry mass of washed leach residue, c_0 is the concentration of an element in the added sulfide concentrate and m_0 is the dry mass of added sulfide concentrate into the experiment. The uncertainty of the ICP-OES analysis was 10%, thus the total uncertainty of the leaching yield was less than 20%. Regarding BR1, the 0% leaching yield for iron was due to the effect of added $FeSO_4 \cdot 7H_2O$ during the ramp-up and precipitation of iron on day 7. For copper, BR1 and BR7 resulted in a calculative leaching yield of 0%.

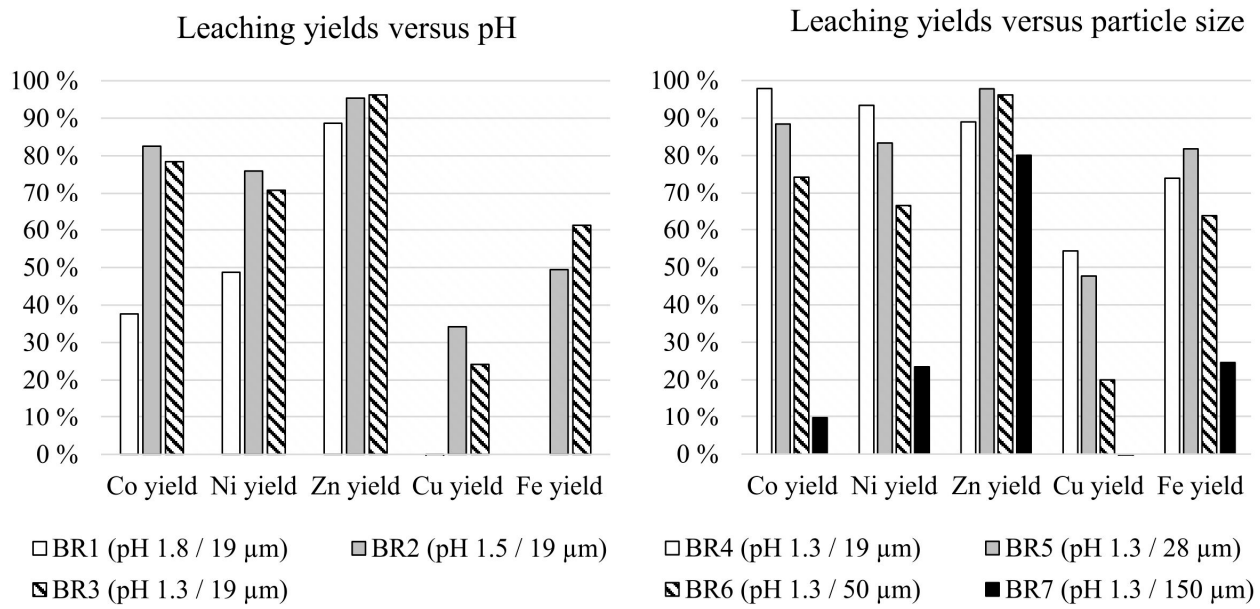

Figure 4. Leaching yields according to the mass balance calculations after 7 days.

4. Discussion

Regarding the bioleaching tests in general, supplemented $FeSO_4 \cdot 7H_2O$ was biologically oxidized to iron(III) in the presence of oxygen (reaction explained by [4]). When the sulfide concentrate was added to reactors, a strong collapse in Eh took place (Figures 1 and 2) due to the reaction between iron(III) and the most reactive sulfide minerals (pyrrhotite, Equation (1); and sphalerite, Equation (2)) [22–24]. As dissolved iron (Figures 1 and 2) and zinc (Figure 3) concentrations continued increasing after the initial collapse of Eh in all tests, pyrrhotite and sphalerite leaching was also continued by acid and oxygen Equations (3) and (4) [25]. This acid dissolution was considered to explain the majority of H_2SO_4 consumption in the ramp-up phase (Table 6).

$$Fe_7S_8 + 14Fe^{3+} \rightarrow 21Fe^{2+} + 8S \quad (3)$$

$$ZnS + 2Fe^{3+} \rightarrow Zn^{2+} + 2Fe^{2+} + S \quad (4)$$

$$Fe_7S_8 + 14H^+ + 3.5O_2 \rightarrow 7Fe^{2+} + 7H_2O + 8S \quad (5)$$

$$ZnS + 2H^+ + 0.5O_2 \rightarrow Zn^{2+} + H_2O + S \quad (6)$$

Some nickel was also dissolving during the ramp-up. The presence of pyrrhotite and sphalerite, as well as relatively low Eh and oxidant concentration, were considered to hinder pentlandite leaching [22,25]. Therefore, some nickel was also present in the pyrrhotite structure and dissolved alongside.

After addition of the sulfide concentrate, the iron(III) oxidant was rapidly reduced in the leaching of the concentrate, with a subsequent collapse of Eh. Microorganisms continued to oxidize iron(II) to iron(III). In BR1, BR5 and BR6, reclaiming the high Eh and iron(III) concentration took a longer time than in BR2, BR3, BR4 and BR7. It was shown that no major iron(III) precipitation took place in BR1, BR5 or BR6 during the ramp-up, as the concentrations of total iron in the leachate and total acid dissolving iron in the pulp were similar, thus we concluded that the low iron(III) concentration was due to less active performance of iron-oxidizing microorganisms. As no clear trends between iron(III) oxidation kinetics and different sulfide concentrate particle sizes were found, the slow ramp-up with some reactors was considered to not completely link to operating parameters, but to the nature of the sulfide concentrate itself. When 50 g/L of pyrrhotite rich material was suddenly added to reactors as a single batch, the iron(III)/iron(II) ratio was switched ex-

tremely rapidly from one opposite to the other (Equation (1), Figures 1 and 2). It is known that at a high iron(III)/iron(II) ratio, *Leptospirillum ferrooxidans* takes over the bioleaching culture from *Acidithiobacillus ferrooxidans*, which dominates cultures at low-to-moderate iron(III)/iron(II) ratios [26]. As the bioreactors reached high Eh and iron(III)/iron(II) by oxidizing supplemented $FeSO_4 \cdot 7H_2O$, it was possible that *L. ferrooxidans* was already dominating the culture. However, the remaining active *A. ferrooxidans*, or their higher amount in some reactors (now already individual despite identical inoculation) may have played the key role in adaptation to the sudden addition of the sulfide concentrate. However, regarding the BR1 ramp-up phase, the pH was occasionally outside the optimal area for both *A. ferrooxidans* and *L. ferrooxidans* (reviewed by [27]), which may have caused some inhibition. However, inhibition was not observed with BR2, which also had elevated pH peaks during ramp-up. The challenging nature of pyrrhotite-containing sulfide concentrate for batch-wise experiments was observed already during adaptation, and by [24]. Therefore, the S/L ratio in these tests was only 50 g/L, and the experimental day 0 for bioleaching was set to +810 mV, to allow equal conditions for pyrite leaching in all reactors.

Cobalt and the majority of nickel started to dissolve when approaching the end of the ramp-up phase (Figure 3). This was explained by their presence as more recalcitrant sulfides, namely cobalt-bearing pyrite and pentlandite. These minerals require higher oxidative power to dissolve, and the oxidation order hinders their dissolution before pyrrhotite and sphalerite [22,25]. In this research, the efficient leaching of pyrite (cobalt) and pentlandite (nickel) was enabled by the exhaustion of sphalerite, Eh > + 800 mV and a concentration of iron(III) >15 g/L. During the active dissolution of pyrite, sulfur was biologically oxidized to sulfuric acid (reactions explained by [4,5]), seen as major consumption of $CaCO_3$ (Table 6) to maintain the target pH. The pH control with $CaCO_3$ was considered important in providing microorganisms a continuous carbon source, as the implemented aeration was not enriched by CO_2 [3].

Cobalt-, nickel- and iron-leaching yields were clearly higher at lower pH levels (Figure 4). This was explained by the higher Eh and iron(III) and sulfuric acid concentration observed in tests BR2 and BR3 compared to BR1. In BR1, the calculative iron leaching yield was 0%, which was explained by the initially added $FeSO_4 \cdot 7H_2O$. On day 7, the majority of iron (both dissolved from the sulfide concentrate and externally added) precipitated from the leachate. It is expected that iron precipitated as ammonium and/or hydronium jarosite at the operating pH and temperature were relatively close to the formation area of jarosite [28], and the nutrient solution contained plenty of $(NH_4)_2SO_4$ (Table 1). For copper, the calculative leaching yield gave 0% recovery at pH 1.8 (BR1). This was controversial when compared to the dissolution rate (Figure 3), where copper was seen to dissolve even more rapidly in BR1 than in BR2 and BR3. Possible explanations for the low calculative copper-leaching yield in BR1 could link to major iron precipitation on day 7 and the related coprecipitation of copper. Moreover, as iron precipitation resulted in the major increase of leach residue mass, and copper had relatively low concentration in the leachate, analytical uncertainties (approximately 10%) may have had a significant effect on the results. Generally, chalcopyrite is prone to passivation in bioleaching operations at the temperatures suitable for mesophiles and high Eh and iron(III) concentrations, therefore resulting in poor leaching yields. Thus, chalcopyrite processes have been proposed to operate at higher temperatures and/or at lower Eh, from +650 mV to +850 mV (reviewed by [29]). However, chalcopyrite dissolution is challenging to increase with the material studied here, as low Eh was shown to decrease the cobalt-leaching yield. For zinc, all pH levels gave rather similar leaching yields, probably as sphalerite dissolves rapidly already at Eh +300 mV [22].

Regarding the additional milling and resulting particle size of the sulfide concentrate, cobalt, nickel and copper yields increased when the particle size decreased, reaching the maximum at d80 < 19 µm (BR4; Figure 4). Even the minor milling (BR6; 60 min of milling resulting in d80 < 50 µm) was highly beneficial for leaching yields compared to the unmilled native sample (BR7). These observations were explained by an activating effect of milling, including an increased surface area and lattice strain, but a decreased crystallite

size [30]. The lack of mechanical activation also caused a clear decrease in iron dissolution (Figures 2 and 4), despite an equal Eh between the unmilled and milled sulfide concentrate tests. This hindered cobalt dissolution even more; when less iron(III) was provided for leaching, pyrite leaching was slower and cobalt was not efficiently exposed to leaching chemicals. However, milling into d80 < 19 µm did not anymore improve the iron-leaching yield, but even decreased it slightly compared to d80 < 28 µm.

Zinc was observed to behave differently compared to other studied metals, as d80 < 50 µm already was clearly enough for efficient leaching. This was logical, as zinc was not present as incorporated into the recalcitrant minerals, but as easily dissolving sphalerite, thus having a more efficient leaching time compared to other target metals. Interestingly, the zinc-leaching yield (Figure 4) was rather similar in pH tests (BR1–BR3) and particle-size tests (BR4–BR6), while the dissolution rate (Figure 3) showed major differences in maximal zinc release from material between the test series. However, all zinc-dissolution curves in BR1–BR6 leveled after day 0, signaling that all zinc was dissolved. While zinc dissolution rate differences looked systematic between BR1–BR3 and BR4–BR6, the difference was considered to be caused by inoculation. As zinc was the only easily dissolving metal, even relatively small differences in cultivation time may have affected the sphalerite dissolution rate in the inoculum, thus making the leachate calculations inaccurate. For other target elements, these differences were not observed, as they were incorporated in recalcitrant minerals, thus their dissolution was hardly started during inoculum cultivation. The inoculum may also explain why BR3 and BR4 had differences, even though they had the same parameters. BR3 obtained the inoculum from the first reactor inoculum batch, while BR4 was from the second reactor inoculum batch. As the second cultivation batch was regrown from the first inoculum batch, tolerance for reactor conditions (agitation and aeration, compared to earlier adaptation in flasks) may have increased.

A small particle size has been occasionally reported as inhibitory for bioleaching microorganisms (reviewed in [14,15]. However, in an earlier study with the same microbial culture as used here, the operation was successful at particle size d80 < 13 µm [19]. In this research, indisputable evidence of inhibition was not observed when the particle size was decreased. However, BR5 (d80 < 28 µm) reached the highest iron(III) concentration in the leachate, and had a slightly higher Eh (Figure 2), compared to BR4 (d80 < 19 µm). Nevertheless, BR4 (d80 < 19 µm) resulted in the highest cobalt- and nickel-leaching yields, thus being the optimal in overall performance.

5. Conclusions

Bioleaching of a polymetallic sulfide concentrate was studied in stirred-tank reactors at 35 °C and a solid/liquid ratio of 50 g/L. The operation at pH 1.8 was prone to iron(III) precipitation and had less active performance of iron-oxidizing microorganisms than operation at pH 1.3–1.5. Additional milling of the native sulfide concentrate (d80 < 150 µm) was required to reach an efficient leaching process.

While in this study the highest cobalt- and nickel-leaching yields were observed with milling to d80 < 19µm, the economic optimum may be something different. It is worth mentioning that decreasing the particle size from d80 < 28 µm to d80 < 19 µm required remarkably more milling, which is considered costly and did not increase metal-leaching yields any more dramatically.

In conclusion, the integration of mechanical activation with acid bioleaching of the polymetallic sulfide concentrate was clearly successful, and we propose to continue testing in continuous mode to overcome the technical challenges regarding rapid dissolution and pH increase due to the initial pyrrhotite leaching. For continuous-mode operation, we propose to operate the system at pH 1.3–1.5 and highlight the need of additional milling to reach d80 < 19–28 µm. Regarding the chemical consumption, we expect usage of 650 kg $CaCO_3$ per ton of dry material, while H_2SO_4 usage should be clearly less than in this study and should be required only in the primary leaching tank due to the steady-state conditions provided by the continuous operation.

Author Contributions: Conceptualization, J.M.; Formal analysis, J.M., T.H., M.S. and P.K.; Investigation, J.M., T.H., and M.S.; Methodology, J.M. and T.H.; Supervision, P.K.; Validation, J.M.; Writing—original draft, J.M., T.H., M.S. and P.K. All authors have read and agreed to the published version of the manuscript.

Funding: This work was supported by the European Commission Horizon 2020 project NEMO "Near-zero-waste recycling of low-grade sulfidic mining waste for critical-metal, mineral and construction raw-material production in a circular economy" [Grant Agreement number 776846], https://h2020-nemo.eu/ (accessed on 2 January 2021).

Data Availability Statement: Not applicable.

Conflicts of Interest: The authors declare no conflict of interest.

References

1. Riekkola-Vanhanen, M. Talvivaara mining company—From a project to a mine. *Miner. Eng.* **2013**, *48*, 2–9. [CrossRef]
2. Neale, J.; Seppälä, J.; Laukka, A.; Van Aswegen, P.; Barnett, S.; Gericke, M. The MONDO Minerals Nickel Sulfide Bioleach Project: From Test Work to Early Plant Operation. *Solid State Phenom.* **2017**, *262*, 28–32. [CrossRef]
3. Morin, D.H.R.; D'hugues, P. Bioleaching of a Cobalt-Containing Pyrite in Stirred Reactors. In *Biomining*; Rawlings, D.E., Johnson, D.B., Eds.; Springer: Berlin/Heidelberg, Germany, 2007; pp. 35–54.
4. Sand, W.; Gehrke, T.; Jozsa, P.-G.; Schippers, A. (Bio) chemistry of bacterial leaching—Direct vs. indirect bioleaching. *Hydrometallurgy* **2001**, *59*, 159–175. [CrossRef]
5. Schippers, A.; Jozsa, P.-G.; Sand, W. Sulfur Chemistry in Bacterial Leaching of Pyrite. *Appl. Environ. Microbiol.* **1996**, *62*, 3424–3431. [CrossRef] [PubMed]
6. Brierley, C.L. Biological Processing: Biological Processing of Sulfidic Ores and Concentrates—Integrating Innovations. In *Innovative Process Development in Metallurgical Industry*; Lakshmanan, V., Roy, R., Ramachandran, V., Eds.; Springer: Cham, Switzerland, 2016. [CrossRef]
7. Peek, E.; Barnes, A.; Tuzun, A. Nickeliferous pyrrhotite-waste or a resource? *Miner. Eng.* **2011**, *24*, 625–637. [CrossRef]
8. Falagán, C.; Grail, B.M.; Johnson, D.B. New approaches for extracting and recovering metals from tailings. *Miner. Eng.* **2017**, *106*, 71–78. [CrossRef]
9. Anderson, C.; Napier-Munn, T.; Wills, B. *Wills' Mineral Processing Technology: An Introduction to the Practical Aspects of Ore Treatment and Mineral Recovery*; Elsevier Science & Technology: Amsterdam, The Netherlands; Butterworth-Heinemann: Oxford, UK, 2015.
10. Torma, A.E.; Walden, C.C.; Duncan, D.W.; Branion, R.M.R. The effect of carbon dioxide and particle surface area on the microbiological leaching of a zinc sulfide concentrate. *Biotechnol. Bioeng.* **1972**, *14*, 777–786. [CrossRef]
11. Torma, A.E. The role of Thiobacillus ferrooxidans in hydrometallurgical processes. In *Advances in Biochemical Engineering*; Ghose, T.K., Fiechter, A., Blakebrough, N., Eds.; Springer: Berlin/Heidelberg, Germany, 1977; Volume 6, pp. 1–37. [CrossRef]
12. Miller, P.C.; Rhodes, M.K.; Winby, R.; Pinches, A.; Van Staden, P.-J. Commercialization of bioleaching for base-metal extraction. *Min. Metall. Explor.* **1999**, *16*, 42–50. [CrossRef]
13. Rouchalova, D.; Rouchalova, K.; Janakova, I.; Cablik, V.; Janstova, S. Bioleaching of Iron, Copper, Lead, and Zinc from the Sludge Mining Sediment at Different Particle Sizes, pH, and Pulp Density Using Acidithiobacillus ferrooxidans. *Minerals* **2020**, *10*, 1013. [CrossRef]
14. Bosecker, K. Bioleaching: Metal solubilization by microorganisms. *FEMS Microbiol. Rev.* **1997**, *20*, 591–604. [CrossRef]
15. Mahmoud, A.; Cézac, P.; Hoadley, A.F.A.; Contamine, F.; D'Hugues, P. A review of sulfide minerals microbially assisted leaching in stirred tank reactors. *Int. Biodeterior. Biodegrad.* **2017**, *119*, 118–146. [CrossRef]
16. Blancarte-Zurita, M.A.; Branion, R.M.R.; Lawrence, R.W. Particle Size Effects in the Microbiological Leaching of Sulfide Concentrates by Thiobacillus Ferrooxidans. *Biotechnol. Bioeng.* **1986**, *28*, 751–755. [CrossRef]
17. Torvinen, J. PLS-Liuoksen Ferrianalytiikan Kehittäminen. Oulu University of Applied Sciences. 2015. Available online: http://urn.fi/URN:NBN:fi:amk-201505087053 (accessed on 18 January 2021).
18. Bomberg, M.; Mäkinen, J.; Salo, M.; Kinnunen, P. High Diversity in Iron Cycling Microbial Communities in Acidic, Iron-Rich Water of the Pyhäsalmi Mine, Finland. *Geofluids* **2019**, *2019*. [CrossRef]
19. Mäkinen, J.; Salo, M.; Khoshkhoo, M.; Sundkvist, J.-E.; Kinnunen, P. Bioleaching of cobalt from sulfide mining tailings; a mini-pilot study. *Hydrometallurgy* **2020**, *196*, 105418. [CrossRef]
20. Silverman, M.P.; Lundgren, D.G. Studies on the chemoautotrophic iron bacterium ferrobacillus ferrooxidans. l. An improved medium and a harvesting procedure for securing high cell yields. *J. Bacteriol.* **1959**, *77*, 642–647. [CrossRef] [PubMed]
21. London Metal Exchange. 2020. Available online: https://www.lme.com/ (accessed on 16 December 2020).
22. Riekkola-Vanhanen, M.; Heimala, S. Electrochemical control in the biological leaching of sulfide ores. In *Biohydrometallurgical Technologies*; Torma, A.E., Wey, J.E., Lakshmanan, V.L., Eds.; The Minerals, Metals and Materials Society: Warrendale, PA, USA, 1993; pp. 561–570.
23. Ghassa, S.; Noaparast, M.; Shafaei, S.Z.; Abdollahi, H.; Gharabaghi, M.; Boroumand, Z. A study on the zinc sulfide dissolution kinetics with biological and chemical ferric reagents. *Hydrometallurgy* **2017**, *171*, 362–373. [CrossRef]

24. Altinkaya, P.; Mäkinen, J.; Kinnunen, P.; Kolehmainen, E.; Haapalainen, M.; Lundström, M. Effect of biological pretreatment on metal extraction from flotation tailings for chloride leaching. *Miner. Eng.* **2018**, *129*, 47–53. [CrossRef]
25. Arpalahti, A.; Lundström, M. The leaching behavior of minerals from a pyrrhotite-rich pentlandite ore during heap leaching. *Miner. Eng.* **2018**, *119*, 116–125. [CrossRef]
26. Rawlings, D.E.; Tributsch, H.; Hansford, G.S. Reasons why 'Leptospirillum'-like species rather than Thiobacillus ferrooxidans are the dominant iron-oxidizing bacteria in many commercial processes for the biooxidation of pyrite and related ores. *Microbiology* **1999**, *145*, 5–13. [CrossRef] [PubMed]
27. Rawlings, D.E. Heavy metal mining using microbes. *Annu. Rev. Microbiol.* **2002**, *56*, 65–91. [CrossRef] [PubMed]
28. Babcan, J. Synthesis of jarosite KFe3(SO4)2(OH)6. *Geol. Zb.* **1971**, *22*, 299–304.
29. Watling, H.R. The bioleaching of sulphide minerals with emphasis on copper sulphides—A review. *Hydrometallurgy* **2006**, *82*, 81–108. [CrossRef]
30. Hasab, M.G.; Raygan, S.; Rashchi, F. Chloride–hypochlorite leaching of gold from a mechanically activated refractory sulfide concentrate. *Hydrometallurgy* **2013**, *138*, 59–64. [CrossRef]